Design of a 1-GW Offshore Wind Farm Test System Based on a Separately Aggregated Feeder Model

Bruno W França
Dragan Jovcic
Electrical Engineering Department
University of Aberdeen
Aberdeen, U.K.
bwfranca, d.jovcic@abdn.ac.uk

Jean Mahseredjian
Department of Electrical Engineering
Polytechnique Montréal, Montréal
Quebec, Canada
jean.mahseredjian@polymtl.ca

Abstract—**This paper firstly presents an EMT model for a 10 MW wind turbine using two parallel back-to-back converters, forming the basis for a 100-machine detailed model for a 1 GW wind farm. It further investigates aggregation methods to reproduce the resonant modes of the collection system, revealing that methods based on equivalent feeder length, equal power loss, and weighted voltage difference do not accurately reflect these modes. A new aggregation method based on a transfer function is proposed. It is demonstrated to maintain the main resonant modes while preserving losses and voltage drop of the collection feeders. The study encompasses theoretical analysis, frequency scans, and time-domain simulations, providing flexibility to explore interactions between machines and feeders within a wind farm.**

Index Terms--**offshore wind generation, wind turbine model, aggregation method**

I. Introduction

The significance of wind energy in Europe has increased as it aims for net-zero emissions by 2050, targeting over 500 GW of installed offshore wind power [1]. Future offshore wind farms are expected to be 1-2 GW in size, utilizing 10-15 MW machines and integrating with HVDC due to distance considerations.

Wind Turbines (WTs) with capacities of tens of MW have not been adequately studied in references. Developing suitable models is challenging due to vendors' and clients' trade secrets. Publications from the National Renewable Energy Laboratory provide initial information for the electromechanical model of the Wind Energy Conversion Systems (WECS), with details on the generator project [2]. To the authors' knowledge, comprehensive Electro-Magnetic Transient (EMT) modelling of WECS over 10 MW is lacking in literature.

Simulating offshore wind parks (WPs) with hundreds of WTs is challenging due to the trade-off between the level of detail required to reproduce observed phenomena and computational complexity. Typically, the approach is first to aggregate strings and then cluster them for WP equivalence [3], [4], which is then connected to some equivalent WT model.

If the feeder's resonance modes are not considered separately from the WECS's modes, these modes can be overlooked or misrepresented. The WT controller can suppress feeder resonance within its frequency range, complicating the detection of actual resonance issues in simulations. Investigating separate aggregation techniques for the feeder network also offers flexibility, allowing for independent study from the WT, its controller, and independent on the level of model transparency (white, gray, or black-boxed model), [3].

The following are the main paper's contributions:

- A detailed model of a 10 MW WT representing typical WECS used in offshore applications.
- Evaluation of several known aggregation methods of the feeder-network's resonant modes. Common string aggregation in a daisy-chain or radial topology is adopted.
- A new aggregation method is proposed. Frequency and time domain comparisons demonstrate superior performance in representing resonant modes,

II. Generic Test System of a 10 MW Wind Turbine

For offshore high-power (tens of MW) wind energy conversion systems (WECS), the Type 4 Permanent Magnet Synchronous Generator (PMSG) with a full-scale power converter is commonly used. To achieve the required power with limited-voltage machines, two parallel stator windings or six-phase configurations are typically employed.

A 10 MW Type-4 WECS design is conducted, aiming to provide a generic model. The preliminary data were collected from [2], [5], [6], [7]. The design aims to determine the system parameters in the same model structure of the WECS system available in the renewable library of the EMTP® software [7], [8], but with the addition of the second parallel back-to-back (B2B) converter system depicted in Figure 1. The EMTP® library does not yet have a 2-winding machine model and therefore a single equivalent-power winding is used, feeding both converters. For simplicity, design details about the switching filter and the coupling transformer will not be discussed. The controller for the second B2B converter system is similar to the original EMTP® controller and is not the focus of this paper. The key parameters are summarized in Table I.

This study is funded by RTE (France).

979-8-3315-8138-1

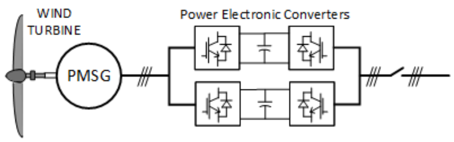

Figure 1: WECS overall diagram.

TABLE I MAIN PARAMETERS FOR THE 10 MW WECS

Parameter	Value	Ref.
Drivetrain model (mechanical parameters)		
Turbine power, P_{WT} (MW)	10.0	[5]
Wind speed, v_w (m/s)	11.24	[7]
Turbine Inertia, H_t, and Generator Inertia, H_g (s)	5.8, 0.9	[5]
Speed deviation damping, K_{sh} (pu/rad)	100.0	[5]
Mutual damping, D_m (pu)	1.0	[5]
PMSG model (electrical parameters)		
Number of poles, P	200	[2]
Generator Frequency (Hz)	50	-
Armature resistance, and leakage reactance (pu)	0.002, 0.05	[7]
Zero-sequence reactance (pu)	0.05	[7]
d-axis, and q-axis self-reactances (pu)	0.6, 0.6	[7]
Turbine and rotor-shaft Frequency (rad/s)	0.8361	
Generator Frequency (Hz)	13.31	
WT Natural Damped frequency (Hz)	1.165	

A. Drivetrain model

The drivetrain is typical of a Type-4 configuration, featuring a direct-drive shaft with no gearbox. The blade radius (R) is calculated using Table I parameters and classical design achieving R = 89.19 m, which is close to the reported value of commercial machines [6]. Standard Cp function can be employed, as provided in the EMTP® simulator [7].

The two-mass model is employed to represent torsional oscillation dynamics and to provide an accurate power oscillation damping profile. Disregarding the turbine and generator friction coefficients, the damped frequency of the free-free rigid shaft torsion mode can be calculated as [5], [9]:

$$f_d = \frac{1}{2\pi}\sqrt{K_{sh}\omega_0\frac{H_t+H_g}{2H_tH_g} - D_m^2\frac{(H_t+H_g)^2}{16H_t^2H_g^2}} = 1.1647\ Hz \quad (1)$$

where ω_0 = 0.8361 rad/s is the mechanical base angular frequency. This frequency was verified in an EMTP® simulation by updating the existing wind turbine model, and a damped frequency of 1.15 Hz was measured.

B. Converter topology and model

A 200-pole machine is adopted, and the generator's electrical frequency is calculated as f_{MSC} = 13.31 Hz, which is close to the design in [2], which has frequency of 14.46 Hz.

Three options are considered for the converter, as summarized in Table II. The largest commercially available IGBTs from INFINEON are considered, with V_{CES} = 4500 V, IC_{DC} = 1800 A, and I_{CRM} = 3600 A, [10]. It is assumed that IGBTs can be connected in parallel, but not in series in a valve. Setting the nominal DC-link voltage approximately to half of the V_{CES}, (V_{dc} = 2300 V for 2-level and V_{dc} = 4600 V for 3-level topology), and adopting the modulation index of M = 0.93 [11], the rated current in semiconductors can be calculated, and also number of parallel converters and IGBTs in valves. We adopted topology 1 as the best trade off, but the other two topologies will have similar average models and give similar results for system-level studies.

DC-link capacitance is calculated for a default energy-to-power ratio of E_s= 30 kJ/MVA (typically from 10 to 50 kJ/MVA), [11]. Each converter has half of the total WT power, S_{conv} = 5 MVA, then $C_{DC} = 2 \cdot S_{conv} \cdot E_s/V_{DC}^2 = 56.71mF$.

TABLE II CONVERTER DESIGN OPTIONS FOR 10MW WT

Parameter	Option 1	Option 2	Option 3
Topology	2L VSC	3L VSC	2L VSC
Converters in parallel	2	2	6
Nominal DC-link voltage (kV)	2.3	4.6	2.3
Generator line-to-line voltage RMS (kV)	1.26	2.62	1.26
Winding AC current RMS (kA)	3.82	1.91	1.27
Number of IGBTs in parallel per valve	3	2	1

III. WIND PARK TEST SYSTEM

The wind park test system configuration shown in Figure 2 includes 100 WT arranged in 20 strings with 5 WT in each radial feeder (daisy-chain). EMT models often simplify complex systems for computation expediency With offshore wind parks, entire strings or groups may be aggregated into a single equivalent turbine, along with a simplified equivalent feeder network, [3], [4], [12].

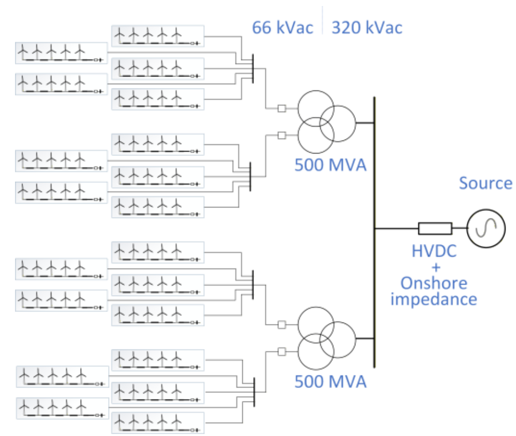

Figure 2: 1 GW wind park test system.

IV. EVALUATION OF AGGREGATION METHODS

We assess aggregation methods by their ability to preserve resonant modes accurately with reduced models. By modeling wind turbines (WT) and feeders separately, we can distinguish the feeder's resonance from WT modes, enabling the identification of inner Sub Synchronous Oscillation (SSO) resonances and the analysis of different feeder topologies. For this reason, WTs (individually or aggregated) are treated as fixed current sources under nominal conditions.

A. String aggregation

A comparison will be made between the full-detailed string model as shown in Figure 3a), and aggregated feeder network equivalent as shown in Figure 3b). The aggregated feeder network is modeled as the Thevenin equivalent impedance of the source and the equivalent PI section cable of the Aggregated-String model.

979-8-3315-8138-1

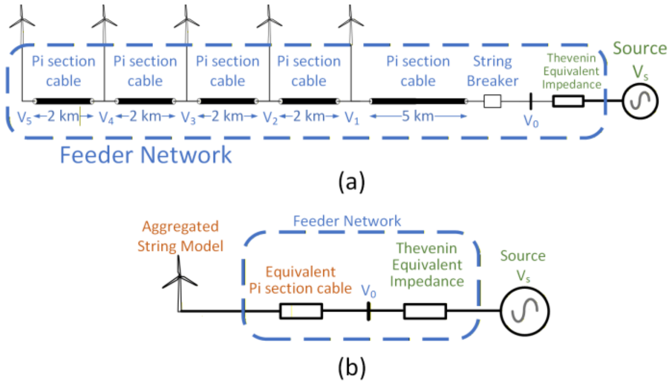

Figure 3: Feeder network (a) full-detailed, and (b) aggregated string.

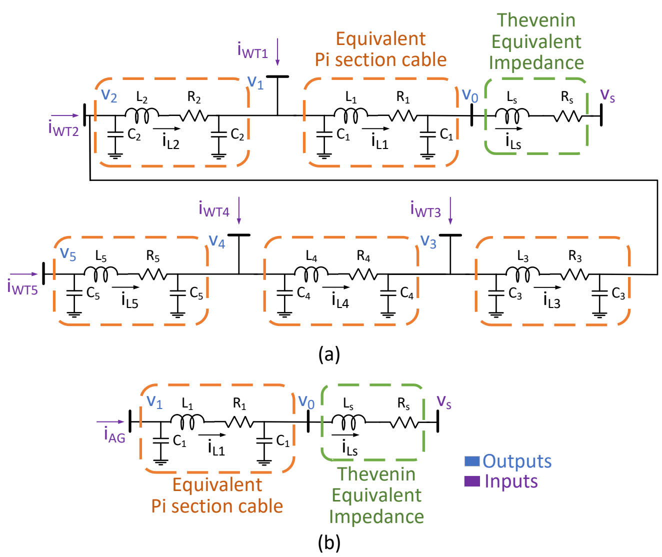

Figure 4: Feeder network diagram (a) full-detailed, and (b) aggregated string.

The complete diagram representing the system of Figure 3 is present in Figure 4a for the full-detailed system (16th-order system) and in Figure 4b for the aggregated string (4th-order system. . The cable is assumed with a cross-section of 500 mm2, AC resistance of 0.05 Ω/km, capacitance per phase of 0.252 µF/km, and inductance per phase of 0.341 mH/km, [13]. For the full-detailed system, the cable length for each section is displayed in Figure 3a. For this string aggregation study, the parameters of the Thevenin equivalent impedance are set for an X/R ratio of 20 and a short-circuit ratio of 2.14, considering the total string nominal power, which leads to L_s = 129.4 mH and R_s = 2.03 Ω for a 66 kV, 50 Hz system.

1) Equivalent length method:

This method sets an equivalent cable length to determine the R_1, C_1, and L_1 parameters, and we will check whether a length accurately represents the original resonant modes. The equivalent length is then assigned to the position of the first turbine (5 km), the midpoint (9 km), and the last turbine (13 km), while considering the same parameter per unit of length. The Bode plot from V_s to V_0 (refer to Figure 4) is used to evaluate the system's resonant modes in both models.

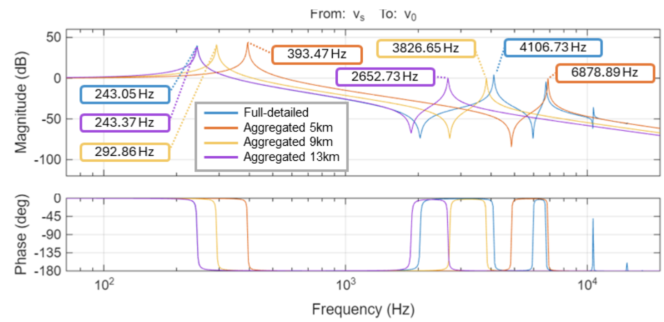

Figure 5: Bode plot for the Equivalent length method.

Figure 5 shows that the frequency responses of the equivalent length model do not match the response of the full-detailed model, and the resonant modes cannot be matched. The first resonant mode frequency (243 Hz) of the 13 km-aggregated model is close to that of the full-detailed model, suggesting that placing the aggregated wind turbine at the end of the daisy chain is optimal for low-resonance compatibility. However, this setup does not match the second resonance mode (4,106 Hz), and adjusting the length to accommodate the second mode compromises the representation of the first mode.

2) Equal Power Loss (EPL) and Weighted Voltage Difference (WVD) methods:

Both EPL and WVD methods result in the same procedure for the adopted daisy-chain with equivalent operational WT configurations. This involves transforming the daisy-chain into a parallel equivalent with impedance feeders, followed by the parallel equivalence of the branch, as presented in Figure 6, [4]. The equations for achieving the equivalent impedance are:

$$Z_{1eq} = \frac{P_1+P_2}{P_1} Z_1;\ Z_{2eq} = \frac{P_1 Z_{1eq}+P_2 Z_2}{P_2};\ Z_{eq} = \frac{Z_{1eq}P_1^2+Z_{2eq}P_2^2}{(P_1+P_2)^2} \quad (2)$$

where $P_{1,2}$ are the active power of the turbines, $Z_{1,2eq}$ are the series equivalent impedances of the transformation from daisy-chained to parallel topology, and Z_{eq} is the equivalent series impedance for aggregation of two turbines. The process is then repeated for all the string's turbines to achieve a single equivalent series impedance, while the equivalent ground capacitance is the sum of the ground capacitance of the string cables.

The procedure was applied to the test system, and the equivalent pi-section cable was achieved with R_1 = 0.3857 Ω; C_1 = 1.638 µF; and L_1 = 2.6304 mH. The Bode plot in Figure 7 indicates that the methods are suitable for matching the first resonant mode but not the second one, and there is an improvement compared to the equivalent length method.

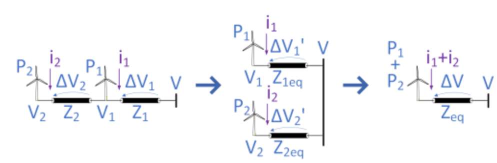

Figure 6: EPL and WVD aggregation method.

979-8-3315-8138-1

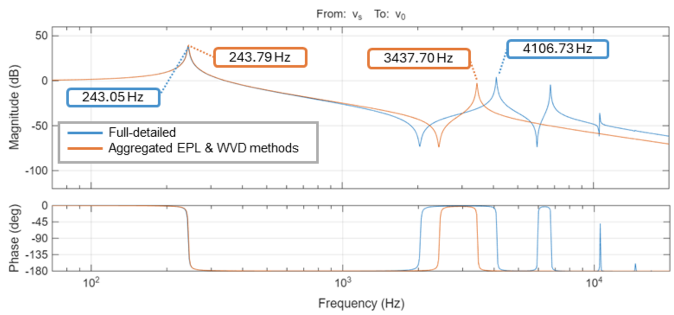

Figure 7: Bode plot for the full-detailed and aggregated feeders based on EPL and WVD methods

V. PROPOSED ESTIMATED TRANSFER FUNCTION (ETF) METHOD:

A. String aggregation using ETF method

This work proposes a new aggregation method, called the Estimated Transfer Function (ETF) method, whose flowchart is depicted in Figure 8. The method relies on the idea that resonance modes can be readily obtained in simple network systems, like radial or daisy-chain topologies.

From the dynamic system (either experimentally or using detailed EMT-type model (FD model)), a frequency-response can be created for specific input/output signals (in the test system, V_s and V_0 were chosen) considering a frequency range of interest. The raw data is then converted to MATLAB sys format using *frd* function. Based on system identification theory, the transfer function can be obtained using the *tfest* MATLAB function. The number of poles and zeros in the transfer function determines the coefficients in the numerator and denominator for comparison with the aggregated transfer function, and they should then be chosen to match the order of the aggregated model's system. All coefficients in the detailed transfer function are numerical, reflecting the desired resonant modes.

The aggregated model (AG) transfer function reflects the circuit structure depicted in Figure 4b. The same mathematical procedure is used to obtain the state-space matrices, with the equivalent pi section cable parameters defined as symbolic variables, as illustrated in Figure 8. Therefore, by choosing the input and output variables, the transfer function of the aggregated model G(s) in the frequency domain is obtained. By comparing the coefficients of the full-detailed transfer function with those of the aggregated transfer function, we derive equations to find the aggregated pi-section cable values that maintain the resonance frequencies. Eliminating unrealistic values and analyzing the Bode plot for these solutions helps in selecting the best parameters for aggregated model.

The proposed ETF method applied to the test system results in an aggregated equivalent pi section cable with $R_1 = 0.2715\ \Omega$, $L_1 = 1.8262$ mH, and $C_1 = 1.6506\ \mu$F. In Figure 9, Bode plots of the reference FD model (the same depicted in Figure 5 and Figure 7), the intermediate estimated FD transfer function (Bode plot from corresponding step in Figure 8), and the final AG model (transfer function of circuit in Figure 4b)), are presented for comparison. The estimated transfer function, considering a frequency range between 10 and 100 kHz, was set using the *tfest* MATLAB function with four poles and two zeros. It is seen that the resonant modes from the aggregated model align well with the full-detailed ones. The selected equations come from the denominators of the transfer functions, with the number of poles and zeros chosen to match the order of the aggregated transfer function. Therefore, the ETF method effectively represents original resonant modes, constrained by the number of modes in the aggregated model.

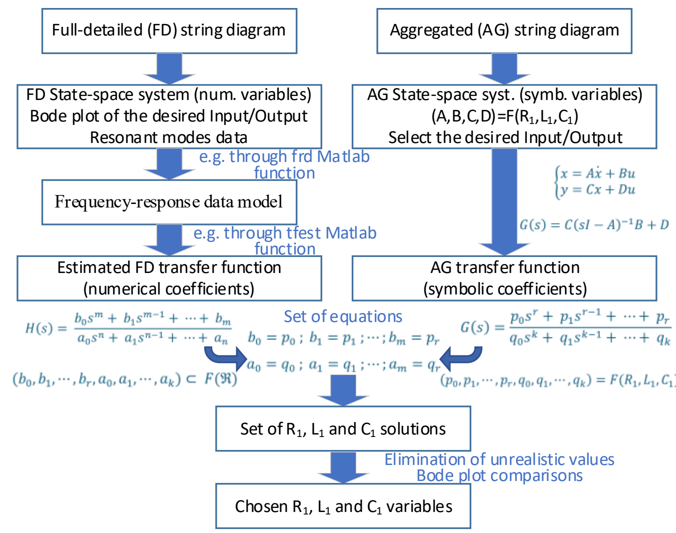

Figure 8: proposed ETF aggregation method.

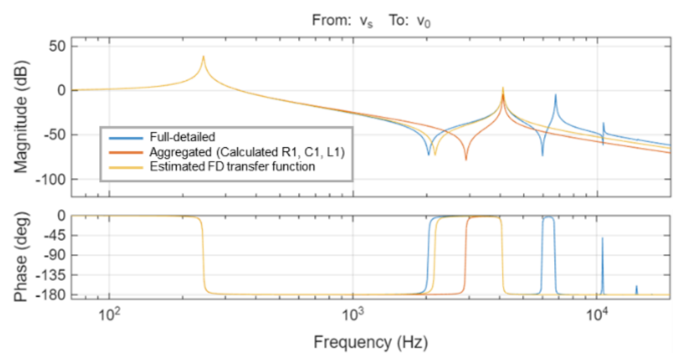

Figure 9: Verification of the aggregated string model using Bode plot.

B. Wind Park aggregation

Parallel aggregation of strings with the same WECS and operational conditions can be performed through EPL or WVD methods without mischaracterizing the resonant modes, assuming that the strings will be subjected to the same conditions. This is the final step in the procedure shown in Figure 6. For n identical pi-section strings (n = 20 in this case study), the aggregation involves dividing the series RL branch by n and multiplying the parallel capacitance by n.

A 1 GW WP test system is proposed with a single Thevenin equivalent impedance representing the substation transformers and source impedances of Figure 2. For the 66 kV, 50 Hz system, with a total 1 GW nominal power, the Thevenin equivalent was set at $R_s = 0.0812\ \Omega$ and $L_s = 6.696$ mH, resulting in an X/R ratio of 25.90 and a short-circuit ratio of 2.07. From the aggregated-string pi cable equivalent circuit obtained in section V.A, the parallel aggregation leads to R_1 = 13.5740 mΩ, L_1 = 91.31 μH, and C_1 = 33.012 μF, and the aggregated WP system equals the diagram of Figure 4b.

The proposed aggregation method will be verified using the EMTP® frequency scan tool, [14]. The WP system's detailed model, including Thevenin equivalent impedance for substation transformers and source impedance, along with the test system for WP aggregated parameters, were simulated using an impedance scan block at bus V_0. A frequency step of 1 Hz was performed, ranging from 1 to 20 kHz. As shown in the frequency scan in Figure 10, the full-detailed system and the proposed aggregated system have the same frequencies and similar damping of both the first and second modes, achieving an aggregated model that accurately represents the resonant modes of the full-detailed mode.

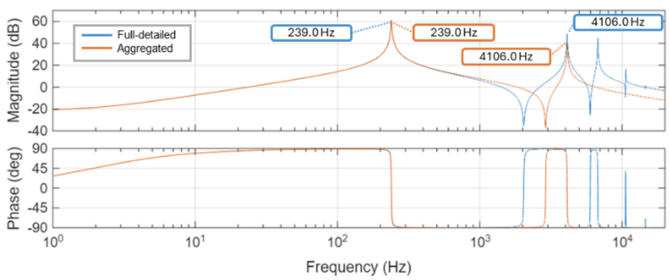

Figure 10: EMTP® frequency scan verification of the proposed model.

C. Time-Domain Simulation Results

A time-domain simulation was conducted to compare the proposed transfer function method with the EPL and WVD methods, taking the full-detailed system as reference. A 0.1 pu voltage step was applied in the V_s source. In Figure 11, the responses of the aggregated methods closely match the full-detailed ones, with a Normalized Sum of Squared Errors of $1.3x10^{-7}$ for the proposed ETF and $7.6x10^{-7}$ for the EPL and WVD methods, computed to the current signals from 1.0 to 1.25s. Note in the zoomed frames that the proposed ETF method is more effective in following the voltages and current profiles, which demonstrates a better adherence due to the modes' compatibility.

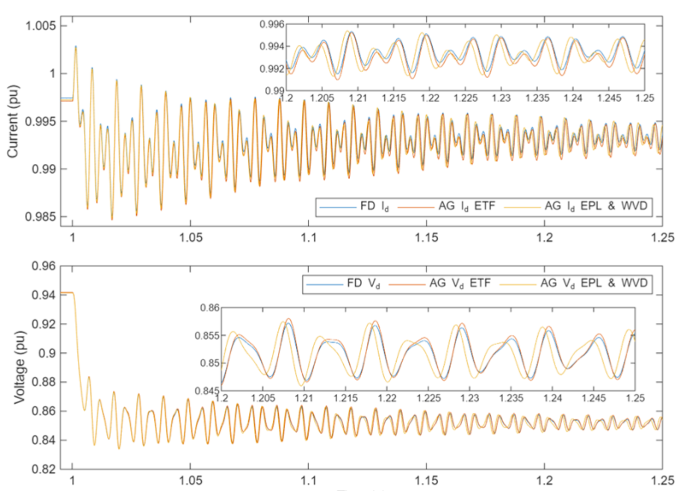

Figure 11: Currents and voltages at bus V_0 during a 0.1 pu voltage step at V_s.

VI. Conclusion

This paper presents the design of a generic 1 GW (100x10 MW) test system that accurately represents the individual 10MW WECS commonly used in offshore applications. The study assessed the equivalent length, EPL, and WVD aggregation methods for string aggregation but found that they inadequately represented the first two resonant modes of the full-detailed reference model that an equivalent pi-section cable can represent. In contrast, the proposed ETF method derives the transfer function from the frequency response and effectively represents the resonant modes while adhering closely to the full-detailed system response. Additionally, this flexible method can apply to other equivalent modes beyond the pi-section cable, suggesting avenues for future research.

References

[1] M. Hjelmeland and J. K. Nøland, 'Correlation challenges for North Sea offshore wind power: a Norwegian case study', *Sci Rep*, vol. 13, Dec. 2023, doi: 10.1038/s41598-023-45829-2.

[2] P. Bortolotti *et al.*, 'IEA Wind TCP Task 37 Systems Engineering in Wind Energy-WP2.1 Reference Wind Turbines Technical Report', 2019. [Online]. Available: www.nrel.gov/publications.

[3] M. K. Bakhshizadeh, B. Vilmann, and Ł. Kocewiak, 'Modal Aggregation Technique to Check the Accuracy of the Model Reduction of Array Cable Systems in Offshore Wind Farms', *Energies (Basel)*, vol. 15, no. 21, Nov. 2022, doi: 10.3390/EN15217996.

[4] C. Guo, F. Gan, D. Du, Y. Guo, and H. Cheng, 'Applicability Evaluation of Wind Farm Impedance Models Using Different Aggregation Methods for High Frequency Oscillation Analysis', *IEEE Transactions on Power Delivery*, vol. 39, pp. 2231–2241, 2024,

[5] Z. Zhang, X. Zhao, L. Fu, and M. Edrah, 'Stability and Dynamic Analysis of the PMSG-Based WECS with Torsional Oscillation and Power Oscillation Damping Capabilities', *IEEE Trans Sustain Energy*, vol. 13, pp. 2196–2210, Oct. 2022, doi: 10.1109/TSTE.2022.3188442.

[6] L. Bauer, 'Siemens Gamesa SG 10.0-193 DD', https://en.wind-turbine-models.com/turbines/1969-siemens-gamesa-sg-10.0-193-dd.

[7] U. Karaagac, H. Ashourian, A. Stepanov, H. Gras, and J. Mahseredjian, 'Wind Park and Wind Turbine Models in EMTP ®', Accessed: Sep. 01, 2025. [Online]. Available: https://emtp.com/documents/EMTP-Documentation/doc/renewables/wind-park-and-wind-turbine-models.pdf

[8] J. Mahseredjian, S. Dennetière, L. Dubé, B. Khodabakhchian, and L. Gérin-Lajoie, 'On a new approach for the simulation of transients in power systems', *Electric Power Systems Research*, vol. 77, no. 11, pp. 1514–1520, Sep. 2007, doi: 10.1016/J.EPSR.2006.08.027.

[9] G. Abad, J. López, M. A. Rodríguez, L. Marroyo, and G. Iwanski, 'Doubly Fed Induction Machine: Modeling and Control for Wind Energy Generation', *Doubly Fed Induction Machine: Modeling and Control for Wind Energy Generation*, Sep. 2011, doi: 10.1002/9781118104965.

[10] I. T. AG, 'FZ1800R45HL4_S7 | 4500 V, 1800 A single switch IGBT module - Infineon Technologies', https://www.infineon.com/cms/en/product/power/igbt/igbt-modules/fz1800r45hl4_s7/.

[11] D. Jovcic, *High Voltage Direct Current Transmission*. Wiley, 2019. doi: 10.1002/9781119566632.

[12] H. Wang, I. Vieto, and J. Sun, 'A Method to Aggregate Turbine and Network Impedances for Wind Farm System Resonance Analysis', *2018 IEEE 19th Workshop on Control and Modeling for Power Electronics, COMPEL 2018*, Sep. 2018, doi: 10.1109/COMPEL.2018.8460155.

[13] 'Submarine Cable Datasheet: Technical Specs & Ratings'. Accessed: Sep. 24, 2025. [Online]. Available: https://studylib.net/doc/27534454/66kv-copper-wet-generaldatasheet-rev0

[14] Jean Mahseredjian, 'Input Impedance'. Accessed: Nov. 10, 2025. [Online]. Available: https://emtp.com/documents/EMTP-Documentation/doc/input-impedance/input-impedance.pdf